



## Lanthanides and heavy metals sorption on alginates as effective sorption materials

D. Kołodzyńska\*, D. Fila

Department of Inorganic Chemistry, Faculty of Chemistry, Maria Curie-Skłodowska University, M. Curie Skłodowska Sq. 2, 20-031 Lublin, Poland, Tel. +48 (81) 5375770, email: d.kolodynska@poczta.umcs.lublin.pl (D. Kołodzyńska), Tel. +48 (81) 5377997, email: dominika.fila@poczta.umcs.lublin.pl (D. Fila)

Received 7 January 2018; Accepted 24 August 2018

### ABSTRACT

This paper presents the possibility of using alginates as biosorbents for the removal of representative of the lanthanide group La(III) ions and heavy metals Cd(II) and Cu(II) ions from aqueous solutions. The calcium alginate in the form of beads obtained by the drop method was used. Biosorption was performed by the static method, studying the effects of pH, sorbent mass, phase contact time, initial solution concentration and temperature on the sorption process efficiency. The greatest removal performance was obtained for pH equal 5 and the sorbent mass equal 0.05 g. The maximum amounts of adsorbed metals were equal to 37.59 mg/g for La(III), 20.08 mg/g for Cd(II) and 15.09 mg/g for Cu(II). In order to determine the kinetic and isotherm parameters of the sorption process, the pseudo-first order, pseudo-second order, intra particle diffusion model kinetic equations as well as the Langmuir and Freundlich isotherms were used. Thermodynamic studies show that the sorption process is spontaneous and exothermic. The sorbent was characterized by attenuated total reflectance Fourier transform infrared spectroscopy, scanning electron microscopy and X-ray photo electron spectroscopy. Moreover, the point of zero charge was determined. The results pointed out that calcium alginate beads can find promising applications for removal and recovery of lanthanide's and heavy metals from aqueous effluents.

*Keywords:* Calcium alginate; Carboxyl group; Lanthanum; Heavy metals removal; Biosorption

### 1. Introduction

With the development of modern technology the demand for various types of materials required for their manufacture has increased. This mainly concerns a particular group of elements known as rare earths elements (REEs). The rare earth elements are present in the earth's crust in a significant amount, but their concentration in the extracted ore is low, resulting in high costs of enrichment. Despite that the use of rare earth elements in industry is growing due to their unique electrical, magnetic and optical properties. Nowadays they are associated with every aspect of life. These metals are widely used in such fields as metallurgy, optics, ceramics, permanent magnets, lasers, catalysts and electronics [1–9]. The wide spread use of these elements

causes their accumulation in the environment and presence in the waste waters. Numerous publications report about the toxic effects of rare earth elements for bacteria, animals and plants [6]. Toxic effects on the environment, the high price of most lanthanide's and their broad applications require recovery of these elements from industrial effluents. Hence there is a need to find a suitable and economical method of rare earth elements recovery from aqueous solutions [1,10,11].

The most common methods of rare earth elements, radio nuclides and heavy metals removal from aqueous solutions are chemical precipitation, ion exchange, filtration, reverse osmosis, electrolysis and adsorption [12,13]. These methods vary mainly in efficiency and costs. Apart from adsorption, they have some disadvantages, such as high operating costs, poor selectivity, high consumption of chemicals and energy or production of secondary metabolites. Therefore,

\*Corresponding author.

it becomes necessary to find more economical and environmentally friendly methods [1,3,6,14,15].

It has been shown that biosorption is a very efficient and effective method for removing heavy metals and rare earth elements from the dilute aqueous solutions. In addition, biosorption has gained an advantage over the conventional methods due to its low cost, simplicity of design and ease of use. Therefore investigations are focused on the preparation of new, low cost and more efficient sorption materials [1,4,16–19].

Among the natural polymers, one of the promising biosorbents is an alginate. It is a well-known polysaccharide obtained from marine algae, mainly brown algae (*Phaeophyceae*) or produced extracellularly by some bacteria, such as *Azotobacter vinelandii*, *Pseudomonas aeruginosa* or *Pseudomonas fluorescens* [2,20].

The original structure of the alginate depends on the source of the marine algae (algae species, seasonal variation and geographical origin) or type of bacteria that produce them [20–22]. Alginate is a water-soluble linear polysaccharide consisting of residues of  $\beta$ -D-mannuronic acid (M blocks) and  $\alpha$ -L-guluronic acid (G blocks) linked together by  $\beta$ -1,4 glycosidic bonds [6,18,23,24]. These blocks M and G can be present in various proportions and various arrangements along the chain (for example MMM, GGG and MGM). From an industrial and biotechnological points of view, the most important feature of alginate is associated with its ability to bind effectively the cations in the second oxidation state, such as Ca(II), Sr(II) and Ba(II). This property leads to the formation of hydrogels (Fig. 1).

Alginate also forms gels with other metal ions which are in different oxidation states, for example Fe(III) and Cr(III). The free carboxyl groups present in both G and M subunits have the ability to form complexes with metal cations. The result of this is the creation of structures resembling an “egg box” [25]. These properties make that alginates can be used for removal of heavy metals and rare earth elements from waste waters. In addition, alginate is preferred over other materials because of its natural origin, biodegradability and being harmless for the environment. The interaction of alginates with calcium ions was used for the design and manu-

facture of the active dressings [16,20,26]. It is also a polymer used in the drug delivery systems, cell encapsulation as well as food and cosmetic industries [27].

The present work focuses on examining the application of calcium alginate beads as a metal sorbent for the disposal of aqueous solutions containing metals such as lanthanum, cadmium and copper obtained from the suitable metal salts. La(III), Cd(II) and Cu(II) ions sorption was studied in the batch system. Influence of pH, sorbent mass, contact time, initial concentration and temperature on the biosorption process was investigated. The equilibrium biosorption data were calculated using the Langmuir and Freundlich isotherm models. In this study surface morphology and chemical composition of biosorbent were studied.

## 2. Materials and methods

### 2.1. Materials

Sodium alginate (ROTH) and calcium chloride hexahydrate  $\text{CaCl}_2 \cdot 6\text{H}_2\text{O}$  (Chempur) were used to prepare calcium alginate beads. Standard solutions of lanthanum(III) ions were prepared from a 1000 mg/L standard solution  $\text{La}(\text{NO}_3)_3$  (Romil Pure Chemistry). Cadmium(II) and copper(II) ions solutions were prepared from cadmium(II) nitrate salt  $\text{Cd}(\text{NO}_3)_2$  and copper(II) chloride dihydrate  $\text{CuCl}_2 \cdot 2\text{H}_2\text{O}$  (Avantor Performance Materials Poland S.A.), respectively. In order to adjust the pH of the metal ions solutions, sodium hydroxide (Avantor Performance Materials Poland S.A.) and hydrochloric acid (Chempur) solutions were used. All the solutions were prepared using distilled water. In this paper all reagents were of analytical grade.

### 2.2. Methods

#### 2.2.1. Preparation of calcium alginate beads

1% solution of sodium alginate was prepared by dissolving 1 g of sodium alginate powder (ROTH) in 100 mL of ultrapure water with continuous stirring (350 rpm) at

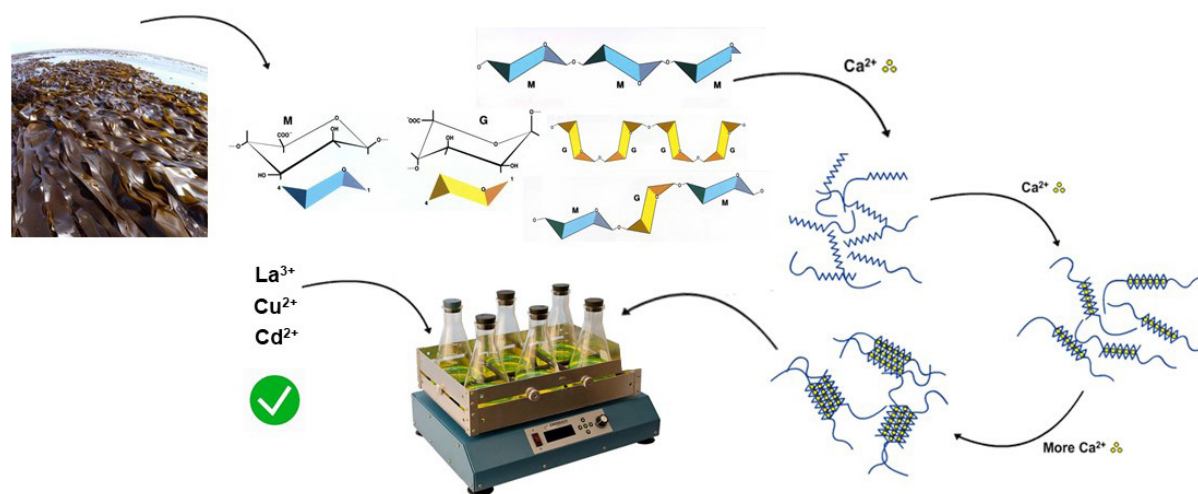


Fig. 1. Alginate hydrogel formation.

room temperature (293 K). After complete dissolution, the sodium alginate solution was added dropwise using a peristaltic pump (type PP1 B-05A, Zalimp) to a 2% solution of calcium chloride at the flow rate 2.5 mL/min. The beads were left in the calcium chloride solution for 24 h. Then they were washed several times with distilled water. The presence of chloride ions was checked using the 0.1 M AgNO<sub>3</sub> solution. The calcium alginate beads were left for a few days to dry at room temperature and then put in a plastic bottle.

### 2.2.2. Sorbent characterization

Fourier Transform Infrared (FTIR) spectroscopy using the ATR (Attenuated Total Reflectance) technique was applied to identify specific functional groups present in the calcium alginate beads. For this purpose the Agilent Cary 630 FTIR spectrometer was employed. Infrared spectra were recorded in the range of 4,000–650 cm<sup>-1</sup>. Spectrum measurements were performed for the calcium alginate beads before and after La(III) ions sorption. The zero point of charge (pH<sub>pzc</sub>) of the alginate beads was determined by the pH drift and potentiometric titration methods using the analytical set of precise titration Dosino, Titrand (Metrohm, Swiss). The pH drift method is commonly applied [28]. The 100 mL volumetric flasks were used in this study. The pH values (pH<sub>0</sub>) of the 0.01 M NaCl solutions were in the range 2–12. The samples of calcium alginate beads (0.5 g of dry weight) were shaken in 50 mL of the 0.01 M NaCl solution for 24 h using a laboratory shaker with the rate of 180 rpm. Then the pH of these solutions was determined (pH<sub>1</sub>). The difference between the pH<sub>0</sub> value and the pH<sub>1</sub> value (pH<sub>1</sub>–pH<sub>0</sub>) was plotted against the pH<sub>0</sub>. The pH value which intersects with the x axis gives pH<sub>pzc</sub> of the sorbent. The morphology of calcium alginate beads before and after adsorption was identified by scanning electron microscopy (SEM, Tescan Vega, USA). The calcium alginate beads were further estimated by the X-ray photo electron spectroscopy (XPS, multi-chamber analytical system UHV, PREVAC, Poland).

### 2.2.3. Preparation of the stock solution

For the studies the stock solutions of metals were prepared. For this purpose a suitable volume of standard solution of La(NO<sub>3</sub>)<sub>3</sub> and a suitable amount of Cd(NO<sub>3</sub>)<sub>2</sub>·4H<sub>2</sub>O and CuCl<sub>2</sub>·2H<sub>2</sub>O salts were added into the 1 L flasks separately. The flasks were filled with distilled water to the mark. The concentration of stock solutions was 100 mg/L.

### 2.2.4. Batch biosorption experiments

Batch biosorption experiments were conducted to find out the most suitable conditions for the biosorption process of metal ions on the calcium alginate beads. Sorption studies were carried out in the defined range of pH, mass of sorbent, contact time of the phases, initial concentration of the solution and temperature. The measurements were performed at room temperature.

The values of pH were determined by the pH-meter (model PHM82 Radiometer, Copenhagen). Batch adsorption experiments were conducted using the laboratory shaker type 358A (Elphin+) with the constant amplitude

of vibration (8) and the constant rate of 180 rpm. Concentrations of lanthanum (III) ions in the solutions were determined by Inductively Coupled Plasma Optical Emission Spectrometry (ICP-OES, 720-ES, Varian). Concentrations of cadmium (II) and copper (II) ions in the solution were determined by Flame Atomic Absorption Spectrometry (FAAS, Spectr AA 240FS, Varian).

The parameter characterizing applicability of the sorbent is the sorption capacity, expressed as the mass of metal ions adsorbed in the dry sorbent mass in relation to the current concentration in the aqueous solution.

The amount of adsorbed metal ( $q_t$ ) was estimated from the following relation:

$$q_t = (C_0 - C_t) \times \frac{V}{m} \quad (1)$$

where  $q_t$  is the amount of adsorbed metal (mg/g),  $C_0$  is the initial concentration of metal in the solution (mg/L),  $C_t$  is the concentration of metal in the solution after time  $t$  (mg/L),  $V$  is the volume of the solution containing metal ions (L),  $m$  is the mass of dry calcium alginate beads (g).

The percentage of adsorption (%S) is that of metal adsorbed on the calcium alginate beads calculated by the following equation:

$$\%S = \frac{C_0 - C_t}{C_0} \times 100\% \quad (2)$$

The influence of pH (from 1 to 6) on metal ions adsorption was investigated using 0.05 g of calcium alginate beads and 20 mL of 100 mg/L La(III), Cd(II) and Cu(II) of stock solutions. In the same way the influence of sorbent mass was investigated using different masses of the sorbent in the range 0.05–0.2 g. The solutions with the alginate beads were stirred for six hours. Then separation of the ions solution from the sorbent was done by filtration. Finally the concentrations of metals were determined.

The kinetic experiments were performed in 100 mL flasks at 293 K. The samples of calcium alginate beads (0.05 g of dry weight) in the 20 mL prepared solution of metal ions were shaken for fixed time (1, 3, 5, 7, 10, 30, 60, 180, 240 and 360 min). The initial concentration of the metal ions La(III), Cd(II) and Cu(II) was 100 mg/L. The pH of the solution was equal to 5. Then the concentrations of metal ions were analyzed.

In the next step, the impact of initial concentration of the tested ions was investigated. The initial concentrations of each metal were ranged from 50 to 200 mg/L. 0.25 g of the alginate beads was put into the 250 mL Erlenmeyer flask and poured with the 100 mL of the prepared working solution of La(III), Cd(II) and Cu(II). The pH of the solution was maintained at 5. The shaking time was equal to 6 h. The influence of temperature was studied at three selected temperatures (293, 313, 333 K). The test procedure was the same as above.

## 3. Results and discussion

### 3.1. Characterization of alginate beads

The ATR-FTIR analysis provides information about the functional groups of the sorbent responsible for the mecha-

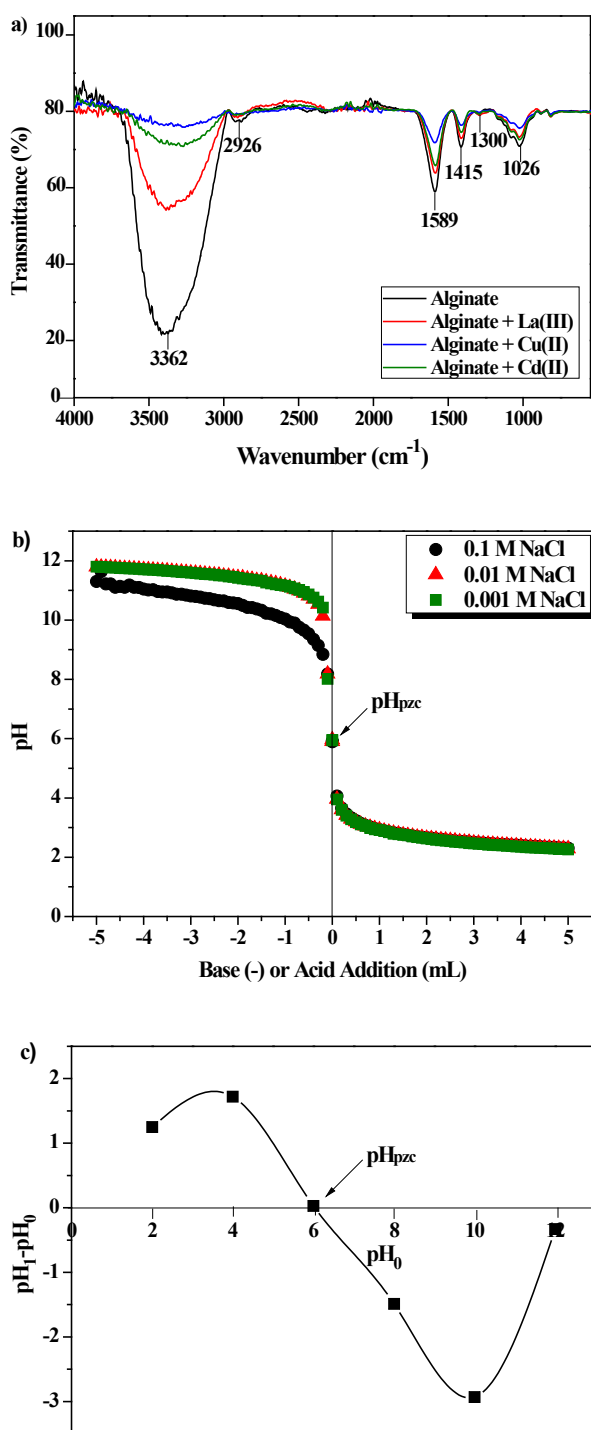


Fig. 2. a) FTIR spectra of calcium alginate beads before and after Cd(II), Cu(II) and La(III) ions sorption and  $\text{pH}_{\text{pzc}}$  of calcium alginate for b) potentiometric titration and c) drift method.

nism of biosorption. Fig. 2a presents the ATR-FTIR spectra of the alginate before and after La(III) ions sorption. On the spectrum a band of  $3,362\text{ cm}^{-1}$  was observed which corresponds to the stretching vibrations of OH groups present in the structure of the alginate [29–31]. The band at  $2,926\text{ cm}^{-1}$  was due to the stretching vibrations in the  $-\text{CH}$  and  $-\text{CH}_2$

groups [32]. The bands at  $1,589$  and  $1,415\text{ cm}^{-1}$  correspond to the asymmetric and symmetric stretching vibrations of C-O group in the  $-\text{COO}^-$  one. These bands confirm the presence of the carbonyl group in the sorbent [33,34]. The spectrum showed other bands at  $1,300$  and  $1,026\text{ cm}^{-1}$  corresponding to the stretching vibrations of C-O-H and C-O-C [35]. After sorption of Cd(II), Cu(II) and La(III) ions slight changes in the shift bands and disappearance of bands were observed. These may be due to the coordination of O atom and metal ions [29,33–36].

The point of zero charge ( $\text{pH}_{\text{pzc}}$ ) is one of the most important parameters for determining surface properties of solids in aqueous solutions. The  $\text{pH}_{\text{pzc}}$  is a pH at which the surface of a solid in water has a zero electric charge. The sorbent surface is negatively charged when this value is below that of pH of solution. This may cause an increase in the removal of metal ions from the solution. In another case, the surface is positively charged and it may promote anion sorption. This point for the calcium alginate beads was obtained by two methods: the drift and potentiometric titration methods. The results are shown in Figs. 2b,c. As follows from the comparison of the two methods, similar values were obtained.  $\text{pH}_{\text{pzc}}$  equal 6.01 was obtained using the drift method and  $\text{pH}_{\text{pzc}}$  5.94 the titration method. Similar values were obtained by Hassan et al. [37,38]. Based on the results it can be concluded that the value of  $\text{pH}_{\text{pzc}}$  of the calcium alginate beads in the water does not depend on the ionic strength.

Scanning electron microscopy (SEM) was used in order to determine morphology of the alginate surface before and after biosorption. The morphology of the alginate beads is presented in Figs. 3a–d.

It can be noticed that the beads have a corrugated structure and rough surface. There can be found unequally distributed nodules with cavities between them on the whole surface showing the ‘eggs-box’ structure, Figs. 3a–d. The SEM results after biosorption of the metal ions onto beads showed a corrugated and weakly heterogeneous surface. The alginate surface after biosorption of La(III), Cu(II) and Cd(II) is rough and porous implying interactions of the metal with the sorbent surface and dislodging of polymer chains.

X-ray photo electron spectroscopy was used in order to determine the interactions between the functional groups on the alginate and the La(III) ions adsorbed and allow the explanation of binding mechanisms. Table 1 shows the composition of the elements and their binding energy in the alginate before and after La(III) biosorption.

Reduction of the percentage composition of Na (from 0.2 to 0%) and Ca (from 3.1 to 2.6%) ions after La(III) ions sorption was observed. Figs. 4a, b show the XPS spectra before and after La(III) sorption. A new peak which appeared at a binding energy  $837.7\text{ eV}$  is due to the presence of La. This confirms sorption of La(III) ions on the alginate and may indicate an ion exchange mechanism during the adsorption process [16]. After the process the intensity of Ca 2p peak decreased. This indicates an ion exchange mechanism. Figs. 4c–d present O 1s spectra for the alginate and alginate + La(III). The peaks at the binding energies  $532.88$  and  $531.58\text{ eV}$  are assigned to the C=O and C-O groups, respectively. After the sorption process these peaks shifted to  $532.58$  and  $531.18\text{ eV}$ , respectively. This may suggest interactions

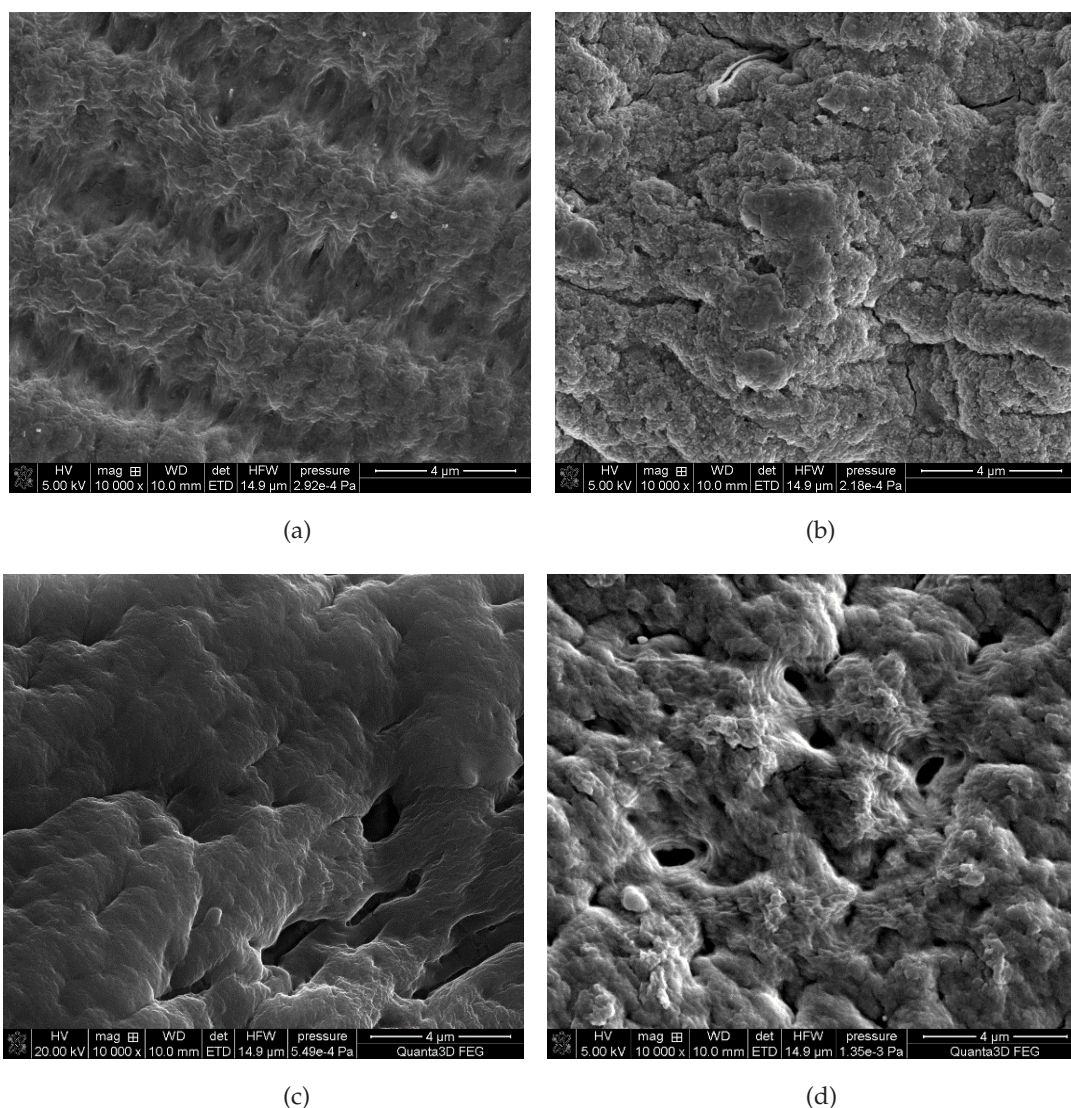


Fig. 3. Morphology of a) calcium alginate beads and b) with La(III), c) Cu(II) and d) Cd(III) ions.

Table 1  
Composition of the elements ( $C_{at}$ ) and binding energy ( $E_B$ ) determined using XPS for unloaded and loaded La(III) calcium alginate beads

Elements	Identification	Alginate		Alginate+La(III)	
		$C_{at}$ (%)	$E_B$ (eV)	$C_{at}$ (%)	$E_B$ (eV)
C 1s	C-C, C-H	63.8	284.7	62.3	284.7
	C-OH, C-O-C		286.3		286.3
	C=O		287.9		287.8
	O=C-O		288.8		288.7
O 1s	C=O, La-O	30.9	531.6	31.9	531.4
	C-OH, C-O-C		533.0		532.8
Ca 2p	Ca 2p <sub>3/2</sub>	3.1	347.5	2.6	347.5
Na 1s	Na <sub>2</sub> CO <sub>3</sub>	0.2	1070.2	–	–
N 1s	N-C=O	2.3	399.2	2.9	399.2
La 3d	La-O	–	–	0.2	837.7

between the carboxyl groups in the alginate with La(III) ions and consequently formation of chemical bonds [34,39,40].

Analogous results were obtained by Oliveira et al. [39]. In this paper there was investigated the mechanism involved in the biosorption process of La(III) on *Sargassum* sp. biomass belonging to brown seaweed. After the biosorption process new peaks appeared at the binding energy 835.2–839.5 eV. They are associated with the presence of La(III). It was shown that the peak at 529.7 eV refers to the interactions of La(III) with oxygen atoms of the chemical groups present on the surface of *Sargassum* biomass.

In the paper by Yu et al. [41] the mechanism of sorption process of Cu(II) on the Fe<sub>3</sub>O<sub>4</sub>-alginate modified biochar microspheres was investigated. It was found that in the case of magnetic microspheres (MM) of calcium alginate (CA) encapsulated biochar (BC) and Fe<sub>3</sub>O<sub>4</sub> after Cu(II) ions sorption, the Ca(II) ions content in MM was reduced. The peaks at 932 eV, 932.5 eV and 951.8, 952.4 eV refer to Cu2p<sub>3/2</sub> and Cu2p<sub>1/2</sub>. Moreover, shift for Cu2p

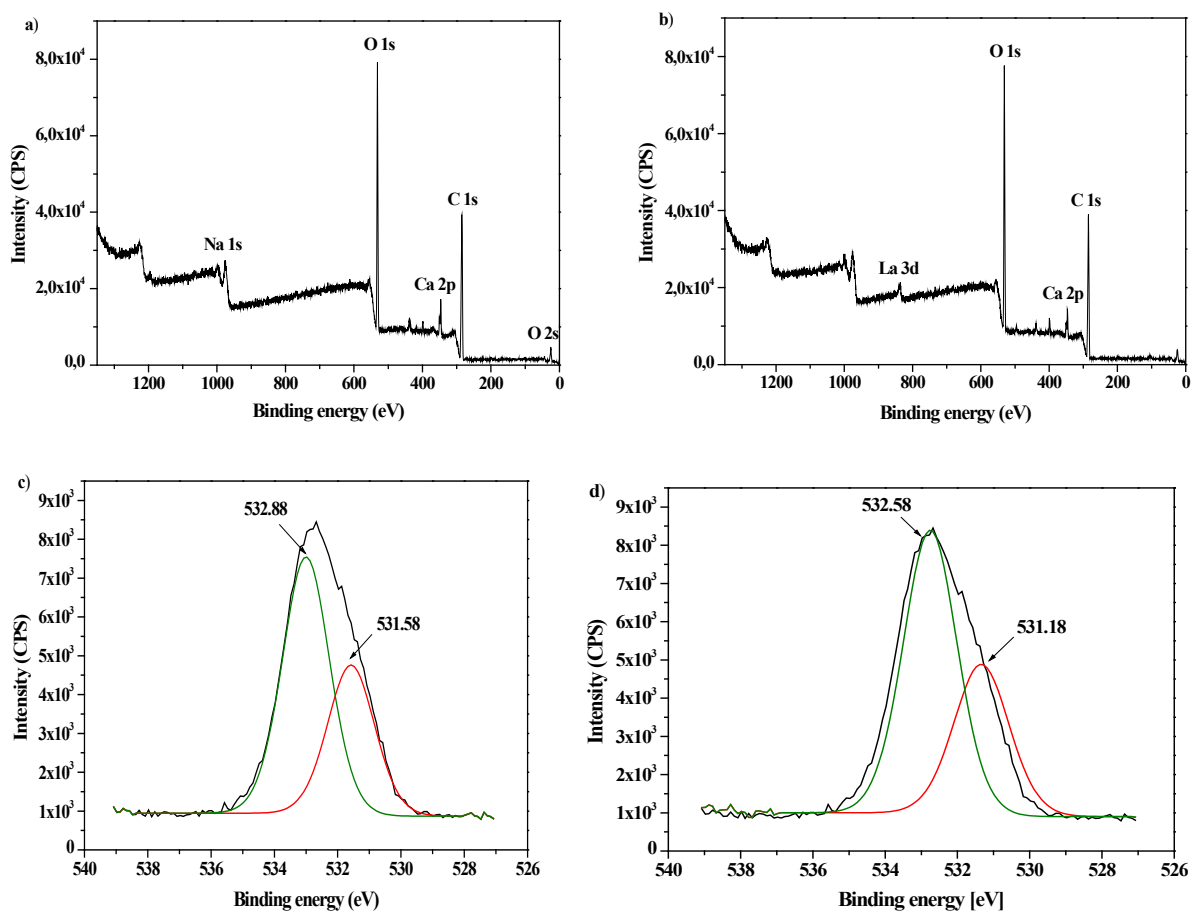


Fig. 4. XPS spectra of calcium alginate a) before and b) after loading of La(III) and O 1s spectra of calcium alginate c) before and d) after La(III) sorption.

to smaller binding energies was observed after Cu(II) adsorption onto MM and MBC. Therefore it can be concluded that coordination/ion exchange is involved for Cu(II) sorption on MM or MBC. Moreover, significant shift for Fe2p to smaller binding energies was also observed after Cu(II) adsorption onto MM, suggesting that the coordination reaction occurs between Cu(II) and  $\text{Fe}_3\text{O}_4$ . The mechanism of Cr(VI) sorption on the sodium alginate-based magnetic carbonaceous biosorbents was also described by Lei et al. [42]. Huang et al. [43] were studied sorption process mechanism of Cu(II) and Pb(II) ions on the ethylenediamine-modified calcium alginate aerogel (ECAA). The spectra analyses indicated that Cu(II) was adsorbed via the chelation of  $-\text{OH}$ ,  $-\text{CO-NH}$  and  $-\text{NH}_2$ . After Cu(II) uptake new peaks at 400.2 eV and at 531.8 eV appeared. It was indicated that the oxygen groups on ECAA were involved in chemisorption of Cu(II) ions. The mechanism of Cu(II) ions on the graphene oxide encapsulated polyvinyl alcohol/sodium alginate hydrogel micro spheres (SPG) was presented by Yi et al. [44]. The main Cu2p peak in the spectrum for SPG after adsorption of Cu(II) ions at 934.1 eV corresponds to Cu(II). The results demonstrated that the Cu(II) ions were attached to the surface of the SPG by ion-exchange or complexation.

### 3.2. Effect of pH

An important parameter affecting the sorption process is pH. Sorption of metal ions onto the calcium alginate depends on pH of the initial solution. This parameter influences the protonation of the carboxyl groups in M and G blocks of the sorbent. The effect of pH on La(III), Cd(II) and Cu(II) ions uptake after 360 min of contact time is illustrated in Fig. 5.

With the increasing pH sorption of these metal ions increases. The maximum sorption capacity was obtained at pH 5 for the tested ions. At this pH, partial deprotonation of the carboxyl groups present in the alginate structure takes place. Thus exchange of hydrogen ions into other metal ions is possible. At  $\text{pH} < 5$ , lower sorption capacity was observed. This is due to the competition between hydrogen ( $\text{H}^+$ ) and metal ions in the solution. For  $\text{pH} \geq 6$  there are observed formation of complex ions and precipitation of metal ions in the form of hydroxides which can lead to decrease of sorption. In this study the solution pH is lower than  $\text{pH}_{\text{pzc}}$  but sorption effectiveness is the highest. This can be explained by the fact that in some cases the surface charge is not so important because other interactions such as the electrostatic ones are more significant. For the investigated metals, the optimum pH for the sorption process was found to be about 5. Therefore this pH value was used in further studies.

### 3.3. Effect of sorbent mass

The second significant parameter influencing on the process is sorbent mass. This parameter is directly related to the sorption capacity for the chosen concentration of

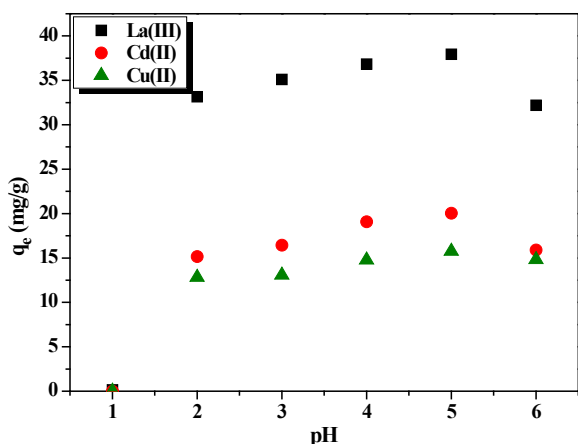


Fig. 5. Comparison of sorption capacity of La(III), Cd(II) and Cu(II) ions depending on pH. Conditions:  $m = 0.05$  g,  $V = 20$  mL,  $C_0 = 100$  mg/L,  $pH = 1-6$ ,  $t = 6$  h,  $T = 293$  K.

metal ions. In order to find an appropriate mass of the sorbent, the experiment was conducted with the alginate mass 0.05–0.2 g, the initial La(III), Cd(II) and Cu(II) ions concentration 100 mg/L and pH of solution 5.0. The effect of adsorbent dosage is presented in Fig. 6. When the sorbent mass increased from 0.05 to 0.2 g, the sorption capacity decreased from 37.21 to 9.38 mg/g for La(III) ions and 20.18 to 4.91 mg/g for Cd(II) ions, but the removal percentage increased from 98.4 to 99.3% for La(III) ions and 44.1 to 50.7% for Cd(II) ions, respectively. The same relation was found for Cu(II) ions. It is considered to be due to the amount of the metal solution which can be insufficient to provide complete coverage of the binding sites present on the sorbent surface, thus causing a slight uptake of sorbate ions. As a result, small changes in the removal percentages compared to those of sorption capacity, 0.05 g sorbent mass was chosen in further experiments.

### 3.4. Sorption kinetics

The sorption kinetics of La(III), Cd(II) and Cu(II) ions by the alginate beads was investigated at the initial pH equal 5.0. Based on the obtained results it can be concluded that with the increasing contact time of phases of the solution-sorbent, the amount of adsorbed metal

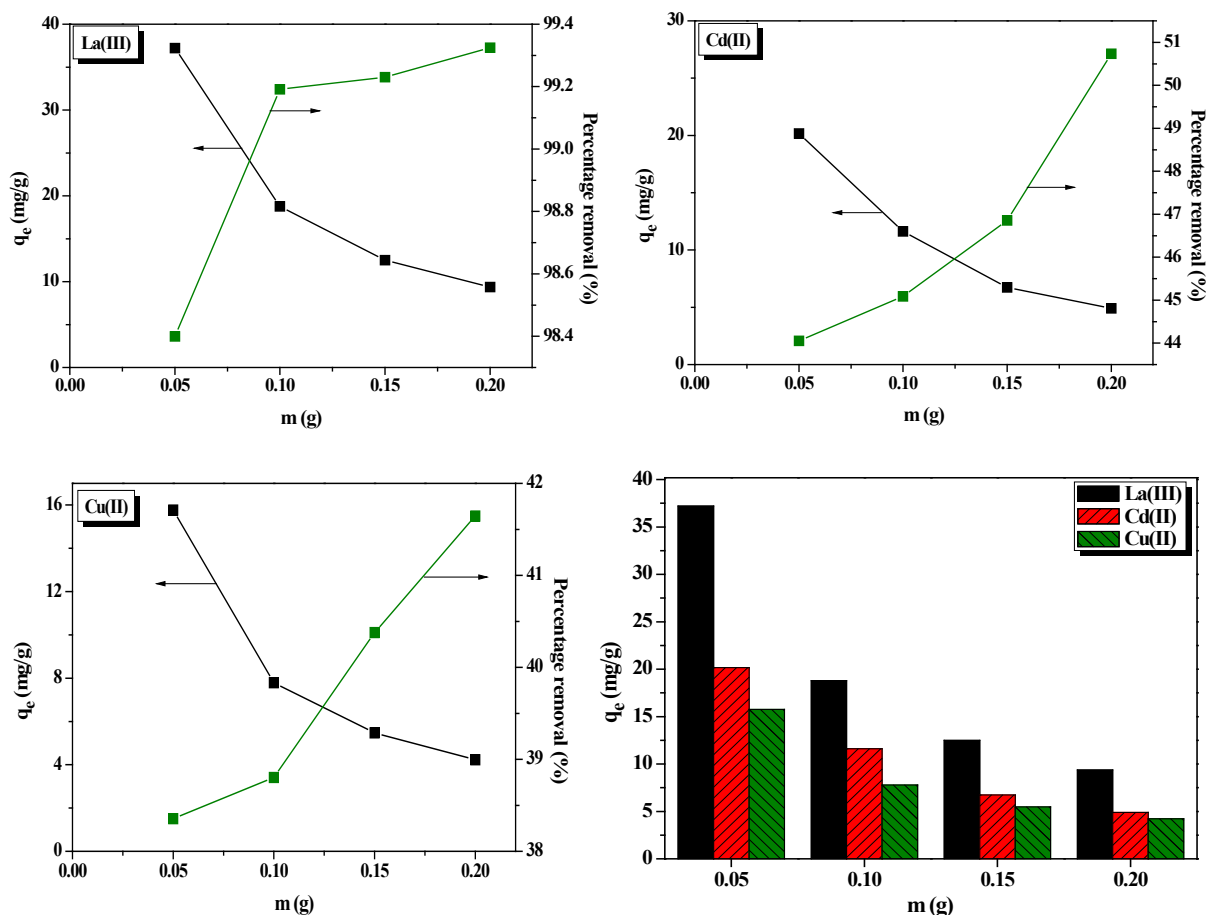


Fig. 6. Effect of adsorbent dosage on La(III), Cd(II) and Cu(II) ions uptake by the calcium alginate. Conditions:  $m = 0.05-0.2$  g,  $V = 20$  mL,  $C_0 = 100$  mg/L,  $pH = 5$ ,  $t = 6$  h,  $T = 293$  K.

ions onto the calcium alginate increases until equilibrium is reached. The kinetic curve for the investigated ions is presented in Fig. 7. It shows that the sorption was initially rapid. The fast adsorption process at the beginning can be due to more accessible sites for adsorption. An equilibrium state was reached after about 180 min. The effectiveness of the sorption process was 99.3% for La(III), 51.1% for Cd(II) and 35.6% for Cu(II) ions. A larger amount of adsorbed metals on calcium alginate was observed for La(III) ions than for Cd(II) and Cu(II) ones. The equilibrium capacities ( $q_e$ ) of the alginate beads were 37.59 mg/g for La(III), 20.18 mg/g for Cd(II) and 15.09 mg/g for Cu(II).

Sorption studies of Cd(II), Cu(II) and La(III) ions on various materials were carried out by many scientists. The adsorption properties of polyaniline Sn(IV) silicate towards Cd(II) ions were studied by Naushad et al. [45]. They revealed that maximum removal of Cd(II) ions occur at pH 9 and equals 89.0%. In another study Naushad et al. [46] synthesized and applied the curcumin formaldehyde resin for the removal of Cd(II) from waste waters. The equilibrium was established after 60 min where 91.2% Cd(II) was adsorbed. The sorption process of Cd(II) ions on  $YVO_4 \cdot Eu^{3+}$  nano particles was also performed by Naushad et al. [47]. In this case the equilibrium state was equal to 90 min. The effectiveness of the sorption process of Cd(II) was 82.0%. Naushad et al. [48] performed sorption of Cu(II) from a synthetic mixture of metal ions: Hg(II), Cd(II), Fe(III), Pb(II), Cu(II) and Zn(II), pharmaceutical and brass alloy samples using the sodium dodecyl sulfate–Th(IV) tungstate (SDS–TT) nano composite cation exchanger. The results indicated the high efficiency and the percentage recovery was more than 83.0% which suggested that SDS–TT was good material for the removal and recovery of Cu(II) in the synthetic and natural samples. Adsorption of rare earth elements i.e. La(III), Nd(III), Eu(III) and actinide Th(IV) from aqueous solutions using graphitic- $C_3N_4$  (g- $C_3N_4$ ) nano sheets was carried out by Liao et al. [49]. The adsorption equilibrium was reached after 420 min and the removal percentages of Eu(III), La(III), Nd(III), Th(IV) was 43.0%, 48.0%, 50.5%, 53.0%, respectively.

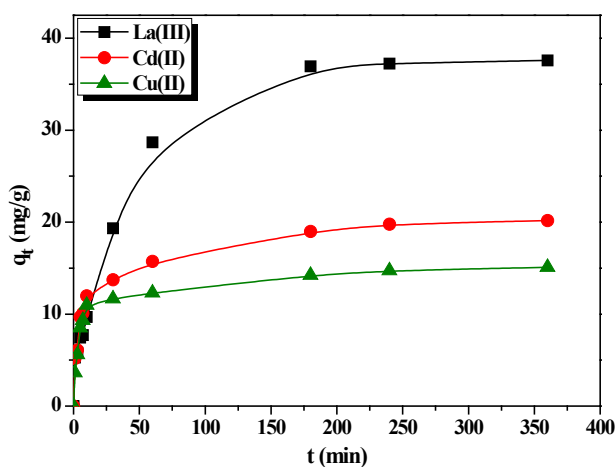


Fig. 7. Influence of contact time on La(III), Cd(II) and Cu(II) sorption process. Conditions:  $m = 0.05$  g,  $V = 20$  mL,  $C_o = 100$  mg/L,  $pH = 5$ ,  $t = 1$ –360 min,  $T = 293$  K.

In order to describe the rate of biosorption process and parameters which confines it, there can be used three kinetic models, which are based on the sorption capacity of the sorbent. Kinetics of La(III), Cd(II) and Cu(II) sorption on the calcium alginate was studied using the pseudo-first order (PFO), pseudo-second order (PSO) as well as Weber and Morris intraparticle diffusion (IPD) models.

Kinetic parameters of metal ions sorption onto the biosorbent were determined using the following equations [50]:

- the pseudo-first order

$$\log(q_e - q_t) = \log(q_e) - \frac{k_1}{2.303} \times t \quad (3)$$

- the pseudo-second order

$$\frac{t}{q_t} = \frac{1}{k_2 \times q_e^2} + \frac{1}{q_e} \times t \quad (4)$$

- the intraparticle diffusion

$$q_t = k_i \times t^{1/2} + C_i \quad (5)$$

where  $q_e$  is the mass of adsorbed metal ions at equilibrium (mg/g),  $q_t$  is the mass of adsorbed metal ions at time  $t$  (mg/g),  $k_1$ ,  $k_2$  and  $k_i$  are the reaction rate constants of the pseudo-first order (1/min), pseudo-second order (g/mg min) and intraparticle diffusion (mg/g min<sup>1/2</sup>) models and  $C_i$  is the intraparticle diffusion constant associated with the boundary layer thickness.

Figs. 8a–c present the curves representing the pseudo-first order, pseudo-second order and intraparticle diffusion models of La(III), Cd(II) and Cu(II) ions sorption. The kinetic parameters of PFO and PSO obtained for the adsorption of metal ions onto the calcium alginate beads are shown in Table 2.

Comparing the data obtained for the pseudo-first order and pseudo-second order equations shows that the sorption process proceeded according to the reaction mechanism typical of the pseudo-second order reaction [51]. This is confirmed by the high values of correlation coefficients  $R^2$ , which were equal to about 0.999. For the pseudo-second order kinetics, the calculated sorption capacities ( $q_{cal}$ ) were consistent with the experimental sorption capacities ( $q_{exp}$ ) for the studied metal ions as shown in Fig. 8b. This indicates that the rate of biosorption process depends more on availability of sorptive sites than on the concentration of metal ions in the solution. Therefore the pseudo-second order mechanism prevails and the chemical adsorption including ion exchange and electrostatic attractions can be the rate limiting step which controls the biosorption process.

However, the pseudo-second order kinetic model observes the biosorption process as a rate-controlling step which does not identify the contribution of diffusion processes. Therefore to provide information about the rate-controlling step of metal ions biosorption, the Weber and Morris intraparticle diffusion model was employed. The determined kinetic parameters of the model are given in Table 3.

The kinetic curves are shown in Fig. 8c. The value of  $k_i$  was calculated from the slope of the plot  $q_t$  vs.  $t^{1/2}$ . The diffusion process and transport into the pores of sorbent is easier

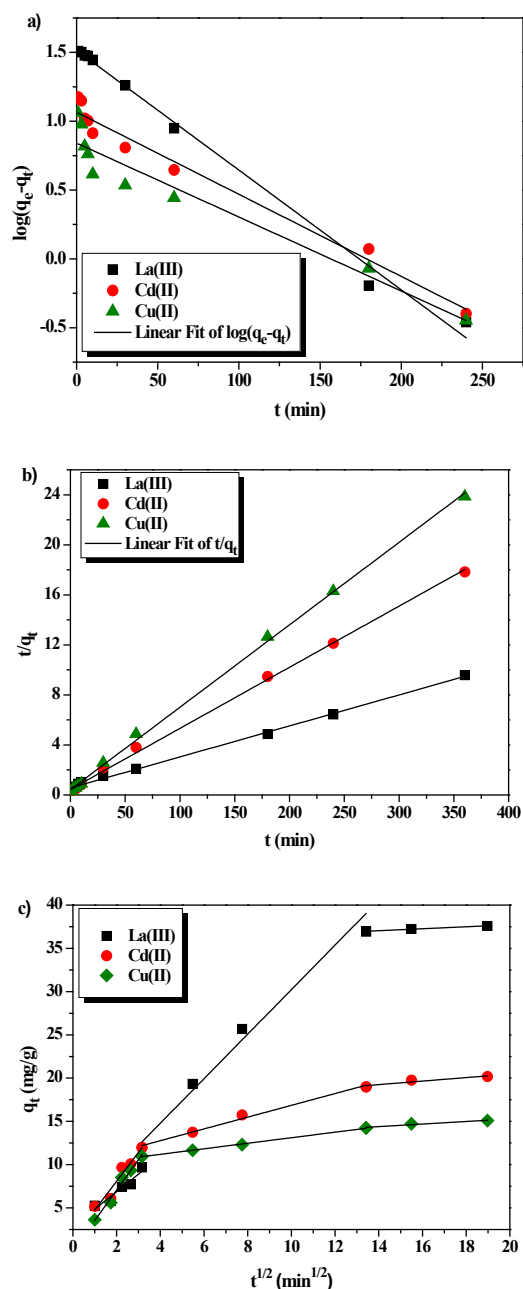


Fig. 8. Biosorption kinetic models: a) pseudo-first order, b) pseudo-second order and c) intraparticle diffusion for sorption process of La(III), Cd(II) and Cu(II) on the calcium alginate beads. Conditions:  $C_0 = 100$  mg/L,  $pH = 5$ ,  $m = 0.05$  g,  $V = 20$  mL,  $t = 1$ –360 min,  $T = 293$  K.

Table 2  
Kinetic parameters of the biosorption process of La(III), Cd(II) and Cu(II) ions onto calcium alginate ( $C_0 = 100$  mg/L)

	Pseudo-first order (PFO)				Pseudo-second order (PSO)		
	$q_{e,exp}$	$q_{1,cal}$	$k_1$	$R^2$	$q_{2,cal}$	$k_2$	$R^2$
La(III)	37.59	32.73	0.020	0.992	40.35	0.001	0.996
Cd(II)	20.18	11.63	0.014	0.978	20.47	0.005	0.999
Cu(II)	15.09	6.93	0.012	0.931	15.17	0.010	0.999

when the  $k_1$  values is greater. From Fig. 8c it can be concluded that the intraparticle diffusion process is a three-step one. The first section corresponds to the rapid adsorption on the outer surface of the sorbent grains, the second section corresponds to the mild adsorption step, in the third section in the final equilibrium step, the intraparticle diffusion starts to decrease due to low concentrations of metal ions in the solution. The obtained curve does not pass through the origin. These results indicate that intraparticle diffusion is not the only mechanism controlling the biosorption rate but can be accompanied by additional mechanisms [52].

### 3.5. Effect of initial concentrations

Another important factor influencing the efficiency of biosorption is the initial concentration of sorbate. The impact of initial concentrations of metal ions (50, 100, 150 and 200 mg/L) on biosorption is illustrated in Figs. 9a–c.

As can be seen, the amount of adsorbed La(III) ions onto the alginate beads is higher than that of Cd(II) and Cu(II) ions at the same concentrations. The adsorption of ions increases sharply at the beginning of the process until equilibrium is reached. It is faster in the initial stages because of greater active sites accessibility on the sorbent surface. Then these sites were occupied by the metal ions and a decrease of active sites for the metal ions remaining in the solution was monitored. An equilibrium is established more rapidly for lower than higher concentrations. At 50 mg/L, equilibrium was reached after 60 min whereas at higher concentrations after approximately 240 min. The results showed that the amount of adsorbed La(III) ions per unit mass of biosorbent increases with the increasing initial concentrations of the metals. With the increase of the initial concentrations of metal ions from 50 to 200 mg/L the amount of adsorbed La(III) ions onto the alginate beads at equilibrium increased from 17.28 to 61.51 mg/g. Similar observations were made for Cd(II) and Cu(II) ions adsorption. In this case, the increase of the initial concentration from 50 to 200 mg/L resulted in an increase of the amount of adsorbed metals at equilibrium from 9.05 to 38.2 and 7.70 to 28.83 mg/g for Cd(II) and Cu(II) ions, respectively.

### 3.6. Adsorption isotherms

At the time of the equilibrium state establishment, distribution of metal ions in both the biosorbent and solution took place. Commonly it is described by means of adsorption isotherm models showing the relation between the amount of the adsorbed substance in the form of ions per unit of mass of sorbent and the equilibrium concentration at constant temperature. The adsorption isotherms are of great

Table 3

Kinetic parameters of the Weber and Morris intraparticle diffusion model for the tested ions ( $C_0 = 100$  mg/L)

	Intraparticle diffusion (IPD)								
	$k_{i,1}$	$C_1$	$R^2$	$k_{i,2}$	$C_2$	$R^2$	$k_{i,3}$	$C_3$	$R^2$
La(III)	2.79	0.986	0.933	2.57	4.481	0.924	0.11	35.451	0.991
Cd(II)	3.33	1.426	0.970	0.68	10.039	0.990	0.20	16.421	0.896
Cu(II)	3.52	0.336	0.991	0.32	9.911	0.998	0.15	12.325	0.944

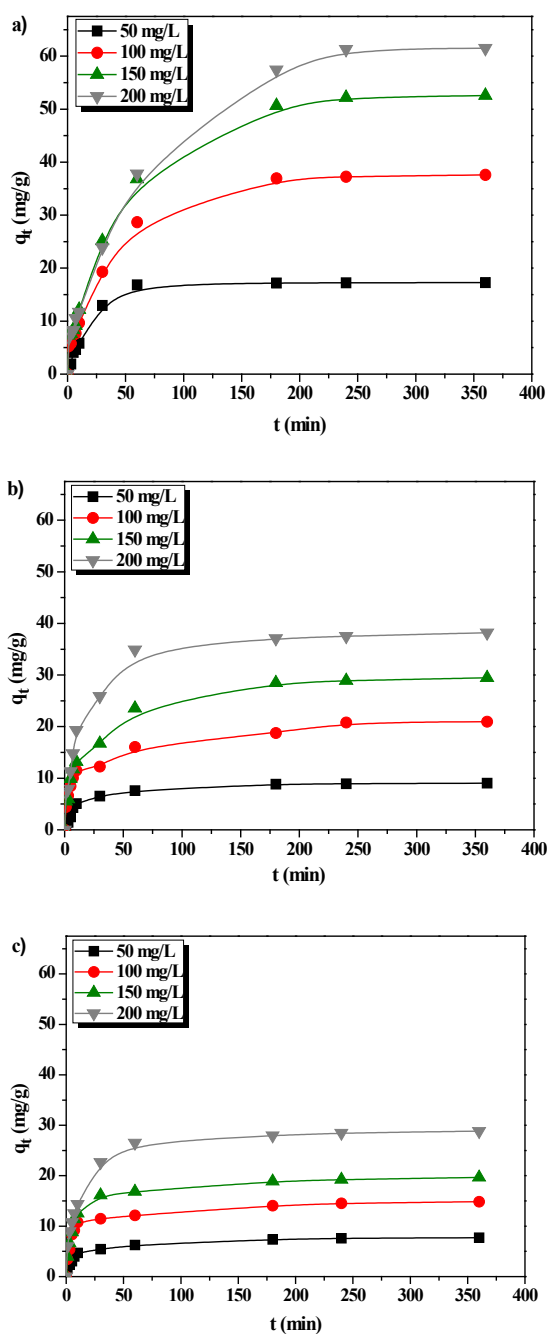


Fig. 9. Influence of initial concentration on metal ions sorption: a) La(III), b) Cd(II) and c) Cu(II). Conditions:  $m = 0.25$  g,  $V = 100$  mL,  $C_0 = 25$ – $200$  mg/L,  $pH = 5$ ,  $t = 1$ – $360$  min,  $T = 293$  K.

importance for investigations of adsorption mechanisms and description of interactions between the adsorbate and the adsorbent. In this paper the Langmuir and Freundlich isotherm models were used to describe the adsorption equilibrium data derived from La(III), Cd(II) and Cu(II) ions adsorption onto the calcium alginate beads. The studied equilibrium adsorption isotherms were of the metal ions concentrations ranging from 50 to 200 mg/L with the solution pH equal 5 and fixed sorbent mass.

The monolayer adsorption theory developed by Langmuir is a commonly used model describing the sorption equilibrium. It assumes that on the sorbent surface the number of active sites capable of binding the adsorbate is defined. Furthermore, no interactions between the adsorbed molecules and the formed monomolecular layer are observed. As a result, the maximum concentration of the surface layer is equal to the number of active sites present on the adsorbent surface. The linear form of the Langmuir model is described as follows [35,53]:

$$\frac{C_e}{q_e} = \frac{C_e}{q_m} + \frac{1}{bq_m} \quad (6)$$

where  $C_e$  are the liquid-phase concentrations of metal ions at equilibrium (mg/L),  $q_e$  is the amount of metal ion adsorbed at equilibrium (mg/g),  $q_m$  is the maximum monolayer adsorption capacity (mg/g) and  $b$  is the Langmuir constant (L/mg).

When the Langmuir equation describes the experimental data, significant importance is the dimensionless separation factor  $R_L$  which it can be determined according to the following equation [38]:

$$R_L = \frac{1}{1 + bC_0} \quad (7)$$

where  $C_0$  is the initial metal concentration. The  $R_L$  parameter predicts the efficiency of the biosorption process. When  $R_L = 0$  the biosorption is irreversible, when  $0 < R_L < 1$  favourable, when  $R_L = 1$  linear and when  $R_L > 1$  unfavourable.

The Freundlich isotherm model determines the adsorption of substances from a liquid to a solid surface. It describes the adsorption equilibrium between the adsorbent in solution and its surface using a multi-site adsorption isotherm for heterogeneous surfaces. The linear form of the Freundlich model is presented as follows [54]:

$$\log q_e = \log K_F + \frac{1}{n} \log C_e \quad (8)$$

where  $C_e$  are the liquid-phase concentrations of metal ions at equilibrium (mg/L) and  $q_e$  is the amount of metal ion adsorbed at equilibrium (mg/g).  $K_F$  and  $1/n$  are the Freun-

dlich constants where  $n$  indicates the degree to which an adsorption process is favourable and  $K_F$  (mg/g (mg/L)<sup>1/n</sup>) is the adsorption capacity of the adsorbent.

The isotherm parameters and the correlation coefficients for biosorption of La(III), Cd(II) and Cu(II) ions onto the calcium alginate are shown in Table 4.

The maximum monolayer adsorption capacities ( $q_m$ ) of La(III), Cd(II) and Cu(II) ions determined from the Langmuir equation were 65.60, 38.36 and 31.87 mg/g, respectively. The parameter  $b$  is a measure of the affinity and efficiency of the biosorption process for the biosorbent. The large value of this parameter indicates a high affinity of the biosorbent for the metal ions (Table 4). Based on the obtained values of the parameter  $b$  it can be concluded that calcium alginate is characterized by greater affinity for La(III) than Cd(II) and Cu(II) ions. The magnitude of  $R_L$  was calculated at 100 mg/L initial metal ions concentration. The obtained values of this factor indicate that the biosorption process is favourable [55]. The high values of correlation coefficients (0.993–0.999) indicate that the biosorption process can be described by the Langmuir model.

Table 4 presents the Freundlich parameters,  $K_F$ ,  $n$  and the correlation coefficient ( $R^2$ ). Biosorption is considered as acceptable when the Freundlich constant takes the values in the range 1–10. The obtained values of this parameter are consistent with the above. The Freundlich constant,  $K_F$  for La(III) ions was the highest compared to the others, pointing out that calcium alginate has the greatest affinity for these ions. The  $R^2$  values are in the range 0.959–0.987 indicating that the biosorption process is better defined by the Langmuir model than the Freundlich one. Based on the adsorption isotherms it can be concluded that the biosorption process of La(III), Cd(II) and Cu(II) ions proceeds favourably onto calcium alginate [56].

### 3.7. Mechanism of sorption process

Calcium alginate beads are characterized good affinity for the tested ions. This is due to the presence of active groups in the alginate structure. They are carboxyl and hydroxyl ones present in the subunits of mannuronic (M) and guluronic (G) acids. Chemical binding of heavy metals with the functional groups can take place by ion exchange, electrostatic attraction or complexation reaction. It was shown that biosorption of multivalent metal ions by the calcium alginate beads occurs predominantly via the ion exchange reaction [57]. This can be caused by electrostatic interactions between the metal cations and the anionic car-

boxyl groups in G and M blocks in the polymer structure [19,26].

The metal ions are exchanged with the calcium ions present in the active groups of alginate according to the following equation:



As can be seen there is a competitive reaction between the  $Ca^{2+}$ ,  $M^{n+}$  and  $COO^-$  groups. Fig. 10 shows a possible binding mechanism of alginate with cations in the second Cd(II), Cu(II) and third La(III) oxidation states. Cadmium(II) and copper(II) ions attach to two  $COO^-$  groups in the alginate, while La(III) ions coordinate with three carboxylic groups.

The results reveal greater affinity of the alginate for La(III) than Cd(II) and Cu(II) ions. Papageorgiou et al. [18] suggested that interactions between the metal ions and ligands are regulated by parameters of metal ions, for example charge and radius [58]. Accordingly, ions with higher charge are preferred by alginates than those with lower charge.

### 3.8. Thermodynamic parameters

The influence of temperature on La(III), Cd(II) and Cu(II) ions sorption on alginate was also investigated. The experiments were performed at 293, 313 and 333 K. Determination of thermodynamic parameters of the sorption process is necessary to understand the process nature. The following parameters: change of Gibbs free energy ( $\Delta G^\circ$ ), change of standard enthalpy ( $\Delta H^\circ$ ) and change of standard entropy ( $\Delta S^\circ$ ) were calculated according to the equations [3,32,45,59]:

$$\Delta G^\circ = -RT \ln K_L \quad (10)$$

$$\Delta G^\circ = \Delta H^\circ - T\Delta S^\circ \quad (11)$$

$$K_L = \frac{q_e}{C_e} \quad (12)$$

$$\ln K_L = \frac{\Delta S^\circ}{R} - \frac{\Delta H^\circ}{RT} \quad (13)$$

where  $R$  is the gas constant  $8.314 \cdot 10^{-3}$  (kJ/mol K),  $K_L$  is the Langmuir constant and  $T$  is the temperature (K).

The Van't Hoff plots were used to measure change of standard enthalpy. The quantities  $\Delta H^\circ$  and  $\Delta S^\circ$  were calculated from the slope and intercept of the plot  $\ln K_L$  vs.  $1/T$ .

The results are given in Table 5. Comparing the amount of adsorbed metal ions at equilibrium at different temperatures, it can be stated that the increase of temperature causes a decrease of the sorption capacity of the alginate relative to the tested metal ions. This can be due to the fact that increasing temperature causes decreasing of adsorptive forces between metal ions and active sites on the sorbent surface causing a decrease in sorption capacity. The thermodynamic calculations indicate the exothermic nature of the sorption process (negative values of  $\Delta H^\circ$ ). The negative values of  $\Delta G^\circ$  at all temperatures indicate that the sorption of La(III), Cd(II) and

Table 4  
Isotherm parameters for biosorption of La(III), Cd(II) and Cu(II) ions onto calcium alginate

Metal ions	Isotherm models					
	Langmuir			Freundlich		
	$q_m$	$b$	$R^2$	$n$	$K_F$	$R^2$
La(III)	65.60	1.328	0.998	2.48	28.67	0.959
Cd(II)	38.36	0.242	0.993	1.71	9.31	0.963
Cu(II)	31.87	0.106	0.999	1.23	4.49	0.987

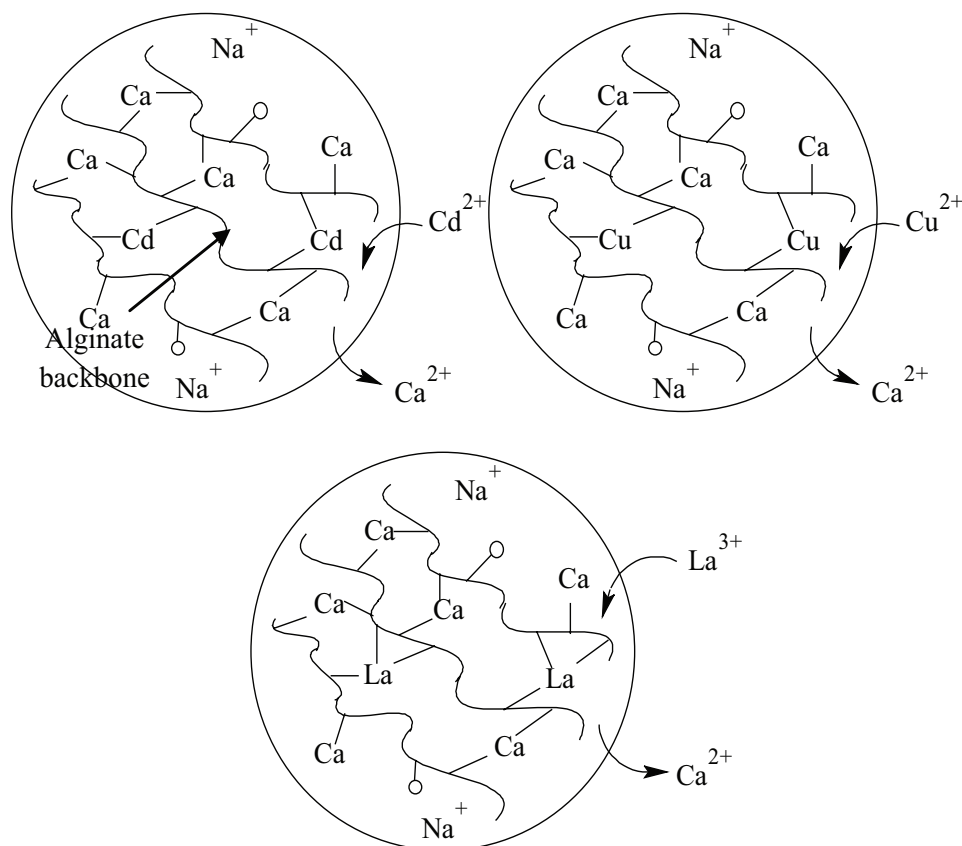


Fig. 10. Probable mechanism of Cd(II), Cu(II) and La(III) ions sorption on alginate.

Table 5  
Thermodynamic parameters of the sorption process of La(III), Cd(II) and Cu(II) ions on calcium alginate

Adsorbed ions	T (K)	$q_e$ (mg/g)	$\Delta H^\circ$ (kJ/mol)	$\Delta S^\circ$ (J/mol K)	$\Delta G^\circ$ (kJ/mol)
La(III)	293	37.59	-42.97	-118.20	-22.77
	313	34.76			-23.90
	333	30.98			-25.19
Cd(II)	293	20.18	-4.21	-24.03	-14.01
	313	16.22			-14.62
	333	12.42			-15.35
Cu(II)	293	15.09	-23.12	-90.79	-11.83
	313	10.76			-12.97
	333	5.98			-13.20

Cu(II) ions is spontaneous and favourable [46]. La(III), Cd(II) and Cu(II) ions after the sorption process are more organized than before as evidenced by the negative value of  $\Delta S^\circ$  [60].

### 3.9. Regeneration studies

Regeneration of the alginate beads was discussed in many papers. For example, the magnetic alginate com-

posite regeneration was greater than 98.6% with 0.01 mol/L HCl. The magnetic alginate composite could be repeatedly utilized for crystal violet removal with a negligible loss in sorption capacity [61]. In the paper by Kumar et al. zirconium oxide (HZO) incorporated into the alginate beads (HZO@AB) adsorbent was effectively reused for three cycles of sorption-desorption of Cr(VI). The adsorption capacity of the regenerated composite adsorbent for Cr(VI) was 6.92 mg/g in the third cycle, and the adsorbent retained approximately 73% of its original Cr(VI) adsorption capacity [62]. Also the percentage of dyes removal after 3 cycles of adsorption-desorption using vineyard-alginate biocomposite formulated with different concentrations of CaCl<sub>2</sub> and 1.25% of cellulosic residue as well as 2.2% of sodium alginate did not change [63]. The desorption experiment was also performed by Wang et al. [64]. The desorption process of Cu(II) and Cd(II) ions from alginate-based attapulgite foam using 0.2 mol/L HCl as a desorption agent was performed. In the first cycle the adsorption capacities of alginate-based ATP foam SP-0.25 for Cu(II) and Cd(II) ions were equal to 73.9 and 75.7 mg/g, respectively. After five cycles the adsorption capacity of sorbent for Cu(II) decreases by 32%. For Cd(II) ions the adsorption capacity increases by 26% and remains unchanged from the second cycle. It was found that these materials have special recyclability for Cu(II) and Cd(II) ions removal.

#### 4. Conclusions

The obtained results showed that the efficiency of the biosorption process affected by the following factors: pH of solution, mass of alginate, contact time of the phases, initial concentration of metal solutions and temperature. The optimal conditions for the sorption process were chosen: pH of solution equal 5, sorbent mass equal 0.05 g, contact time of phases equal 240 min and process temperature equal 293 K. Calcium alginate beads have greater affinity for La(III) ions than for Cd(II) and Cu(II) ones. This indicates preference of higher charge. On the basis of these results the series of affinities were determined: La(III)>Cd(II)>Cu(II). The ATR-FTIR and XPS analyses confirmed the presence of functional groups (carboxyl and hydroxyl) in the alginate structure and interactions of tested ions with oxygen atoms present in the alginate groups. The results indicate that ion exchange is one of the mechanisms found in the biosorption process. La(III), Cd(II) and Cu(II) ions sorption on calcium alginate is the best described by the pseudo-second order kinetic model. Intraparticle diffusion was extremely important although it was not the only step controlling the rate of the whole process. The adsorption equilibrium is best described by the Langmuir isotherm model. Based on the thermodynamic study, the sorption process was of spontaneous and exothermic character. Satisfying results of the process suggest the possibility of using calcium alginate as an effective material for removal of rare earth elements and heavy metal ions from waste waters.

#### References

- [1] N. Das, D. Das, Recovery of rare earth metals through biosorption: An overview, *J. Rare Earths*, 31 (2013) 933–943.
- [2] Z.S. Birungi, E.M.N. Chirwa, The kinetics of uptake and recovery of lanthanum using freshwater algae as biosorbents: Comparative analysis, *Bioresour. Technol.*, 160 (2014) 43–51.
- [3] C. Kütahyalı, Ş. Sert, B. Çetinkaya, S. Inan, M. Eral, Factors affecting lanthanum and cerium biosorption on *Pinus brutia*-leaf powder, *Sep. Sci. Technol.*, 45 (2010) 1456–1462.
- [4] K. Vijayaraghavan, J. Jegan, Entrapment of brown seaweeds (*Turbinaria conoides* and *Sargassum wightii*) in polysulfone matrices for the removal of praseodymium ions from aqueous solutions, *J. Rare Earths*, 33 (2015) 1196–1203.
- [5] K. Vijayaraghavan, M. Sathishkumar, R. Balasubramanian, Biosorption of lanthanum, cerium, europium, and ytterbium by a brown marine alga, *Turbinaria conoides*, *Ind. Eng. Chem. Res.*, 49 (2010) 4405–4411.
- [6] F. Wang, J. Zhao, X. Wei, F. Huo, W. Li, Q. Hu, H. Liu, Adsorption of rare earths(III) by calcium alginate-poly glutamic acid hybrid gels, *J. Chem. Technol. Biotechnol.*, 89 (2014) 969–977.
- [7] M.K. Jha, A. Kumari, R. Panda, J.R. Kumar, K. Yoo, J.Y. Lee, Review on hydro-metallurgical recovery of rare earth metals, *Hydro-metallurgy*, 165 (2016) 2–26.
- [8] G.A. Moldoveanu, V.G. Papangelakis, Recovery of rare earth elements adsorbed on clay minerals: I. Desorption mechanism, *Hydro-metallurgy*, 117–118 (2012) 71–78.
- [9] K. Binnemans, P.T. Jones, B. Blanpain, T. Van Gerven, Y. Yang, A. Walton, M. Buchert, Recycling of rare earths: A critical review, *J. Clean. Prod.*, 51 (2013) 1–22.
- [10] W. Yantasee, G.E. Fryxell, R.S. Addleman, R.J. Wiacek, V. Koonsiripaiboon, K. Pattamakomsan, V. Sukwarotwat, J. Xu, K.N. Raymond, Selective removal of lanthanides from natural waters, acidic streams and dialysate, *J. Hazard. Mater.*, 168 (2009) 1233–1238.
- [11] R.C. Oliveira, O. Garcia Jr., Study of biosorption of rare earth metals (La, Nd, Eu, Gd) by *Sargassum* sp. biomass in batch systems: physico-chemical evaluation of kinetics and adsorption models, *Adv. Mater. Res.*, 71–73 (2009) 605–608.
- [12] M. Naushad, T. Ahamad, B.M. Al-Maswari, A. Abdullah Alqadami, S.M. Alshehri, Nickel ferrite bearing nitrogen-doped mesoporous carbon as efficient adsorbent for the removal of highly toxic metal ion from aqueous medium, *Chem. Eng. J.*, 330 (2017) 1351–1360.
- [13] A. Abdullah Alqadami, M. Naushad, Z. Abdullah Althman, A.A. Ghfar, Novel metal-organic framework (MOF) based composite material for the sequestration of U(VI) and Th(IV) metal ions from aqueous environment, *ACS Appl. Mater. Interfaces*, 9 (2017) 36026–36037.
- [14] K.Z. Elwakeel, A.M. Daher, A.I.L. Abd El-Fatah, H. Abd, E. Monem, M.M.H. Khalil, Biosorption of lanthanum from aqueous solutions using magnetic alginate beads, *J. Dispers. Sci. Technol.*, 38 (2017) 145–151.
- [15] E.-R. Kenawya, A.A. Ghfara, M. Naushadb, Z.A.A.L. Othmanb, M.A. Habilab, A.B. Albadarinc, Efficient removal of Co(II) metal ion from aqueous solution using cost-effective oxidized activated carbon: kinetic and isotherm studies, *Desal. Water Treat.*, 70 (2017) 220–226.
- [16] D. Wu, Y. Gao, W. Li, X. Zheng, Y. Chen, Q. Wang, Selective adsorption of La<sup>3+</sup> using a tough alginate-clay-poly(n-isopropylacrylamide) hydrogel with hierarchical pores and reversible re-deswelling/swelling cycles, *ACS Sustain. Chem. Eng.*, 4 (2016) 6732–6743.
- [17] J.A. Kim, G. Dodbiba, Y. Tanimura, K. Mitsushashi, N. Fukuda, K. Okaya, S. Matsuo, T. Fujita, Leaching of rare-earth elements and their adsorption by using blue-green algae, *Mater. Trans.*, 52 (2011) 1799–1806.
- [18] S.K. Papageorgiou, F.K. Katsaros, E.P. Kouvelos, J.W. Nolan, H. Le Deit, N.K. Kanellopoulos, Heavy metal sorption by calcium alginate beads from *Laminaria digitata*, *J. Hazard. Mater.*, 137 (2006) 1765–1772.
- [19] S.K. Papageorgiou, E.P. Kouvelos, F.K. Katsaros, Calcium alginate beads from *Laminaria digitata* for the removal of Cu<sup>2+</sup> and Cd<sup>2+</sup> from dilute aqueous metal solutions, *Desalination*, 224 (2008) 293–306.
- [20] A. Pielasz, *Algi i alginiany - leczenie, zdrowie i uroda*, Wydawnictwo internetowe e-bookowo, 2010.
- [21] T.A. Davis, B. Volesky, A. Mucci, A review of the biochemistry of heavy metal biosorption by brown algae, *Water Res.*, 37 (2003) 4311–4330.
- [22] G.G. Arantes de Carvalho, S. Kondaveeti, D.F.S. Petri, A.M. Fioroto, L.G.R. Albuquerque, P.V. Oliveira, Evaluation of calcium alginate beads for Ce, La and Nd preconcentration from groundwater prior to ICP OES analysis, *Talanta*, 161 (2016) 707–712.
- [23] F. Wang, J. Zhao, F. Pan, H. Zhou, X. Yang, W. Li, H. Liu, Adsorption properties toward trivalent rare earths by alginate beads doping with silica, *Ind. Eng. Chem. Res.*, 52 (2013) 3453–3461.
- [24] D. Wu, J. Zhao, L. Zhang, Q. Wu, Y. Yang, Lanthanum adsorption using iron oxide loaded calcium alginate beads, *Hydro-metallurgy*, 101 (2010) 76–83.
- [25] Y.N. Mata, M.L. Blazquez, A. Ballester, F. Gonzalez, J.A. Munoz, Biosorption of cadmium, lead and copper with calcium alginate xerogels and immobilized *Fucus vesiculosus*, *J. Hazard. Mater.*, 163 (2009) 555–562.
- [26] B. An, H. Lee, S. Lee, S.H. Lee, J.W. Choi, Determining the selectivity of divalent metal cations for the carboxyl group of alginate hydrogel beads during competitive sorption, *J. Hazard. Mater.*, 298 (2015) 11–18.
- [27] I. Niñá, M. Iorgulescu, M.F. Spiroiu, The adsorption of heavy metal ions on porous calcium alginate micro particles, *Anal. Chem.*, 1 (2007) 59–67.
- [28] J.H. Chen, J.C. Ni, Q.L. Liu, S.X. Li, Adsorption behavior of Cd(II) ions on humic acid-immobilized sodium alginate and hydroxyl ethyl cellulose blending porous composite membrane adsorbent, *Desalination*, 285 (2012) 54–61.

- [29] N. Djebri, M. Boutahala, N.E. Chelali, N. Boukhalfa, L. Zeroual, Enhanced removal of cationic dye by calcium alginate/organobentonite beads: Modeling, kinetics, equilibriums, thermodynamic and re usability studies, *Int. J. Biol. Macro mol.*, 92 (2016) 1277–1287.
- [30] Y. Vijaya, S.R. Popuri, V.M. Boddu, A. Krishnaiah, Modified chitosan and calcium alginate biopolymer sorbents for removal of nickel (II) through adsorption, *Carbohydr. Polym.*, 72 (2008) 261–271.
- [31] M.F. Abou Taleb, D.E. Hegazy, S.A. Ismail, Radiation synthesis, characterization and dye adsorption of alginate-organophilic montmorillonite nano composite, *Carbohydr. Polym.*, 87 (2012) 2263–2269.
- [32] M.A. Khan, W. Jung, O.H. Kwon, Y.M. Jung, K.J. Paeng, S.Y. Cho, B.H. Jeon, Sorption studies of manganese and cobalt from aqueous synthetic solutions by calcium alginate and chitosan coated alginate beads, *J. Ind. Eng. Chem.*, 20 (2014) 4353–4362.
- [33] W.P. Voo, B.B. Lee, A. Idris, A. Islam, B.T. Tey, E.S. Chan, Production of ultra-high concentration calcium alginate beads with prolonged dissolution profile, *RSC Adv.*, 5 (2015) 36687–36695.
- [34] Z. Wang, Y. Huang, M. Wang, G. Wu, T. Geng, Y. Zhao, A. Wu, Macro porous calcium alginate aerogel as sorbent for Pb<sup>2+</sup> removal from water media, *J. Environ. Chem. Eng.*, 4 (2016) 3185–3192.
- [35] N.E. Mousa, C.M. Simonescu, R.E. Pătescu, C. Onose, C. Tardei, D.C. Culiță, O. Oprea, D. Patroi, V. Lavric, Pb<sup>2+</sup> removal from aqueous synthetic solutions by calcium alginate and chitosan coated calcium alginate, *React. Funct. Polym.*, 109 (2016) 137–150.
- [36] S.J. Kleinübing, F. Gai, C. Bertagnolli, M.G.C. da Silva, Extraction of alginate biopolymer present in marine alga *Sargassum filipendula* and bioadsorption of metallic ions, *Mater. Res.*, 16 (2013) 481–488.
- [37] A.F. Hassan, A.M. Abdel Mohsen, H. Elhadidy, Adsorption of arsenic by activated carbon, calcium alginate and their composite beads, *Int. J. Biol. Macromol.*, 68 (2014) 125–130.
- [38] A.F. Hassan, A.M. Abdel Mohsen, M.M.G. Fouda, Comparative study of calcium alginate, activated carbon and their composite beads on methylene blue adsorption, *Carbohydr. Polym.*, 102 (2014) 192–198.
- [39] R.C. Oliveira, P. Hammer, E. Guibal, J.M. Taulemesse, O. Garcia, Characterization of metal-biomass interactions in the lanthanum(III) biosorption on *Sargassum* sp. using SEM/EDX, FTIR, and XPS: Preliminary studies, *Chem. Eng. J.*, 239 (2014) 381–391.
- [40] C. Bertagnolli, A. Uhart, J.C. Dupin, M.G.C. da Silva, E. Guibal, J. Desbrieres, Biosorption of chromium by alginate extraction products from *Sargassum filipendula*: Investigation of adsorption mechanisms using X-ray photo electron spectroscopy analysis, *Bioresour. Technol.*, 164 (2014) 264–269.
- [41] Ch. Yu, M. Wang, X. Dong, Z. Shi, X. Zhang, Q. Lin, Removal of Cu(II) from aqueous solution using Fe<sub>3</sub>O<sub>4</sub>-alginate modified biochar micro spheres, *RSC Adv.*, 7 (2017) 53135–53144.
- [42] Z. Lei, S. Zhai, J. Lv, Y. Fan, Q. An, Z. Xiao, Sodium alginate-based magnetic carbonaceous biosorbents for highly efficient Cr(VI) removal from water, *RSC Adv.*, 5 (2015) 77932–77941.
- [43] Y. Huang, Z. Wang, Preparation of composite aerogels based on sodium alginate and its application in removal of Pb<sup>2+</sup> and Cu<sup>2+</sup> from water, *Int J Biol Macromol.*, 107 (2018) 741–747.
- [44] X. Yi, F. Sun, Z. Han, F. Han, J. He, M. Ou, J. Gu, X. Xu, Graphene oxide encapsulated polyvinyl alcohol/sodium alginate hydrogel micro spheres for Cu(II) and U(VI) removal, *Ecotoxicol Environ Saf.*, 158 (2018) 309–318.
- [45] M. Naushad, Z.A.A.L. Othman, M. Islam, Adsorption of cadmium ion using a new composite cation-exchanger polyaniline Sn(IV) silicate: kinetics, thermodynamic and isotherm studies, *Int. J. Environ. Sci. Technol.*, 10 (2013) 567–578.
- [46] M. Naushad, T. Ahamad, Z.A.A.L. Othman, M.A. Shar, N.S. AlHokbany, S.M. Alshehri, Synthesis, characterization and application of curcumin formaldehyde resin for the removal of Cd<sup>2+</sup> from wastewater: Kinetics, isotherms and thermodynamic studies, *J. Ind. Eng. Chem.*, 29 (2015) 78–86.
- [47] M. Naushad, A.A. Ansari, Z. A. ALOthman, J. Mittal, Synthesis and characterization of YVO<sub>4</sub>:Eu<sup>3+</sup> nano particles: kinetics and isotherm studies for the removal of Cd<sup>2+</sup> metal ion, *Desal. Water Treat.*, 57 (2016) 2081–2088.
- [48] M. Naushad, Z.A. ALOthman, M.M. Alam, M.R. Awual, G.E. Eldesoky, M. Islam, Synthesis of sodium dodecyl sulfate-supported nano composite cation exchanger: removal and recovery of Cu<sup>2+</sup> from synthetic, pharmaceutical and alloy samples, *J. Iran. Chem. Soc.*, 12 (2015) 1677–1686.
- [49] Q. Liao, D. Zou, W. Pan, W. Linghu, R. Shen, X. Li, A.M. Asiri, K.A. Alamry, G. Sheng, L. Zhan, X. Wu, Highly efficient capture of Eu(III), La(III), Nd(III), Th(IV) from aqueous solutions using g-C<sub>3</sub>N<sub>4</sub> nano sheets, *J. Mol. Liq.*, 252 (2018) 351–361.
- [50] P. Staroń, J. Chwastowski, M. Banach, Sorption and desorption studies on silver ions from aqueous solution by coconut fiber, *J. Clean. Prod.*, 149 (2017) 290–301.
- [51] V.S. Munagapati, D.S. Kim, Equilibrium isotherms, kinetics, and thermodynamics studies for congo red adsorption using calcium alginate beads impregnated with nano-goethite, *Ecotoxicol. Environ. Saf.*, 141 (2017) 226–234.
- [52] S. Vishali, P. Rashmi, R. Karthikeyan, Potential of environmental-friendly, agro-based material *Strychnos potatorum*, as an adsorbent, in the treatment of paint industry effluent, *Desal. Water Treat.*, 57 (2016) 18326–18337.
- [53] K. Kondo, K. Hirayama, M. Matsumoto, Adsorption of metal ions from aqueous solution onto micro alga entrapped into Ca-alginate gel bead, *Desal. Water Treat.*, 51 (2013) 4675–4683.
- [54] M.B. Ibrahim, S. Sani, Comparative isotherms studies on adsorptive removal of congo red from wastewater by watermelon rinds and neem-tree leaves, *Open J. Phys. Chem.*, 4 (2014) 139–146.
- [55] M. Naushad, S. Vasudevan, G. Sharma, A. Kumar, Z.A. ALOthman, Adsorption kinetics, isotherms, and thermodynamic studies for Hg<sup>2+</sup> adsorption from aqueous medium using alizarin red-S-loaded amberlite IRA-400 resin, *Desal. Water Treat.*, 57 (2016) 18551–18559.
- [56] Y. Li, F. Liu, B. Xia, Q. Du, P. Zhang, D. Wang, Z. Wang, Y. Xia, Removal of copper from aqueous solution by carbon nano tube/calcium alginate composites, *J. Hazard. Mater.*, 177 (2010) 876–880.
- [57] C. Gok, S. Aytas, Biosorption of uranium(VI) from aqueous solution using calcium alginate beads, *J. Hazard. Mater.*, 168 (2009) 369–375.
- [58] F. Wang, X. Lu, X.Y. Li, Selective removals of heavy metals (Pb<sup>2+</sup>, Cu<sup>2+</sup>, and Cd<sup>2+</sup>) from wastewater by gelation with alginate for effective metal recovery, *J. Hazard. Mater.*, 308 (2016) 75–83.
- [59] Y. Liu, Y.J. Liu, Biosorption isotherms, kinetics and thermodynamics, *Sep. Purif. Technol.*, 61 (2008) 229–242.
- [60] J. Yu, J. Wang, Y. Jiang, Removal of uranium from aqueous solution by alginate beads, *Nucl. Eng. Technol.*, 49 (2017) 534–540.
- [61] K.Z. Elwakeel, A.A. El-Bindary, A.Z. El-Sonbati, A.R. Hawas, Magnetic alginate beads with high basic dye removal potential and excellent regeneration ability, *Canad. J. Chem.*, 88 (2018) 113–121.
- [62] R. Kumar, S.J. Kim, K.H. Kim, S.H. Lee, H.S. Park, B.H. Jeon, Removal of hazardous hexavalent chromium from aqueous phase using zirconium oxide-immobilized alginate beads, *Appl. Geochem.*, 95 (2017) 807–815.
- [63] X. Vecino, R. Devesa-Rey, J.M. Cruz, A.B. Moldes, Study of the physical properties of calcium alginate hydrogel beads containing vineyard pruning waste for dye removal, *Carbohydr. Polym.*, 115 (2015) 129–138.
- [64] Y. Wang, Y. Feng, X-Fei Zhang, X. Zhang, J. Jiang, J. Yao, Alginate-based attapulgite foams as efficient and recyclable adsorbents for the removal of heavy metals, *J. Colloid Interface Sci.*, 514 (2018) 190–98.